



# Highly Efficient Bifunctional Dielectric Metasurfaces at Visible Wavelength: Beam Focusing and Anomalous Refraction in High-Order Modes

Zhenyu Xu, Zhiwei Li\*, Yanqing Tian, Yunbing Wei and Fei Wu

School of Electronic and Electrical Engineering, Shanghai University of Engineering Science, Shanghai, China

## OPEN ACCESS

### Edited by:

Zhi Hong,  
China Jiliang University, China

### Reviewed by:

Elyas Bayati,  
University of Washington,  
United States  
Iliia L. Rasskazov,  
University of Rochester, United States

### \*Correspondence:

Zhiwei Li  
zhiwei.li@sues.edu.cn

### Specialty section:

This article was submitted to  
Optics and Photonics,  
a section of the journal  
Frontiers in Physics

Received: 24 June 2020

Accepted: 07 September 2020

Published: 06 October 2020

### Citation:

Xu Z, Li Z, Tian Y, Wei Y and Wu F  
(2020) Highly Efficient Bifunctional  
Dielectric Metasurfaces at Visible  
Wavelength: Beam Focusing and  
Anomalous Refraction in High-Order  
Modes. *Front. Phys.* 8:575824.  
doi: 10.3389/fphy.2020.575824

Metasurface is an artificially arranged sub-wavelength micro-structure array, where each structure can be regarded as a unit cell that is controlled by electromagnetic waves. Recently, bifunctional metasurfaces have garnered increasing interest and become excellent candidates for device miniaturization and integration. In this study, we propose a highly efficient bifunctional metasurface composed of silicon nanopillars, enabling beam anomalous refraction and focusing at visible wavelength. Based on the proposed metasurface, the other two metasurfaces demonstrating high-order beam anomalous refraction and focusing are designed successfully. This work will establish a positive prospect for the development of high-performance bifunctional metasurfaces.

**Keywords:** metasurface, bifunctional, highly-efficient, high-order, visible band

## INTRODUCTION

The complete control of electromagnetic waves has always been an emerging field of research. Traditional optical equipment has a large volume, heavyweight, complex shape, and other inevitable defects, therefore, such equipment is not suitable for application in integrated photonic systems and device miniaturization. Considering the fact that the conventional optical components rely on gradual phase shifts accumulated during light propagation to shape light beams [1], a three-dimensional metamaterial, exhibits peculiar material properties that do not exist in nature, provide a more flexible way in manipulating the wavefront of electromagnetic waves, which can be used to realize negative refractive index [2], perfect lens [3], and invisibility cloaking [4]. However, three-dimensional metamaterials have many drawbacks, such as high inherent losses and manufacturing difficulties, which limit the miniaturization of the device in practice. With the development of nanotechnology, a metasurface, which is regarded as a two-dimensional metamaterial, has been proposed to cope with the drawbacks due to its ultrathin sub-wavelength structure, relatively easy to manufacture and conformal integration with systems [5, 6]. Metasurfaces typically consist of an array of sub-wavelength metallic or dielectric nanostructures, their geometric parameters, including size, shape, and direction can be adjusted to change the amplitude, phase, and polarization of light. Based on the obvious features, various metasurfaces with different functions have been extensively studied, including beam deflectors [7–10], metalenses [11–13], waveplates [14, 15], and high-resolution holograms [16, 17].

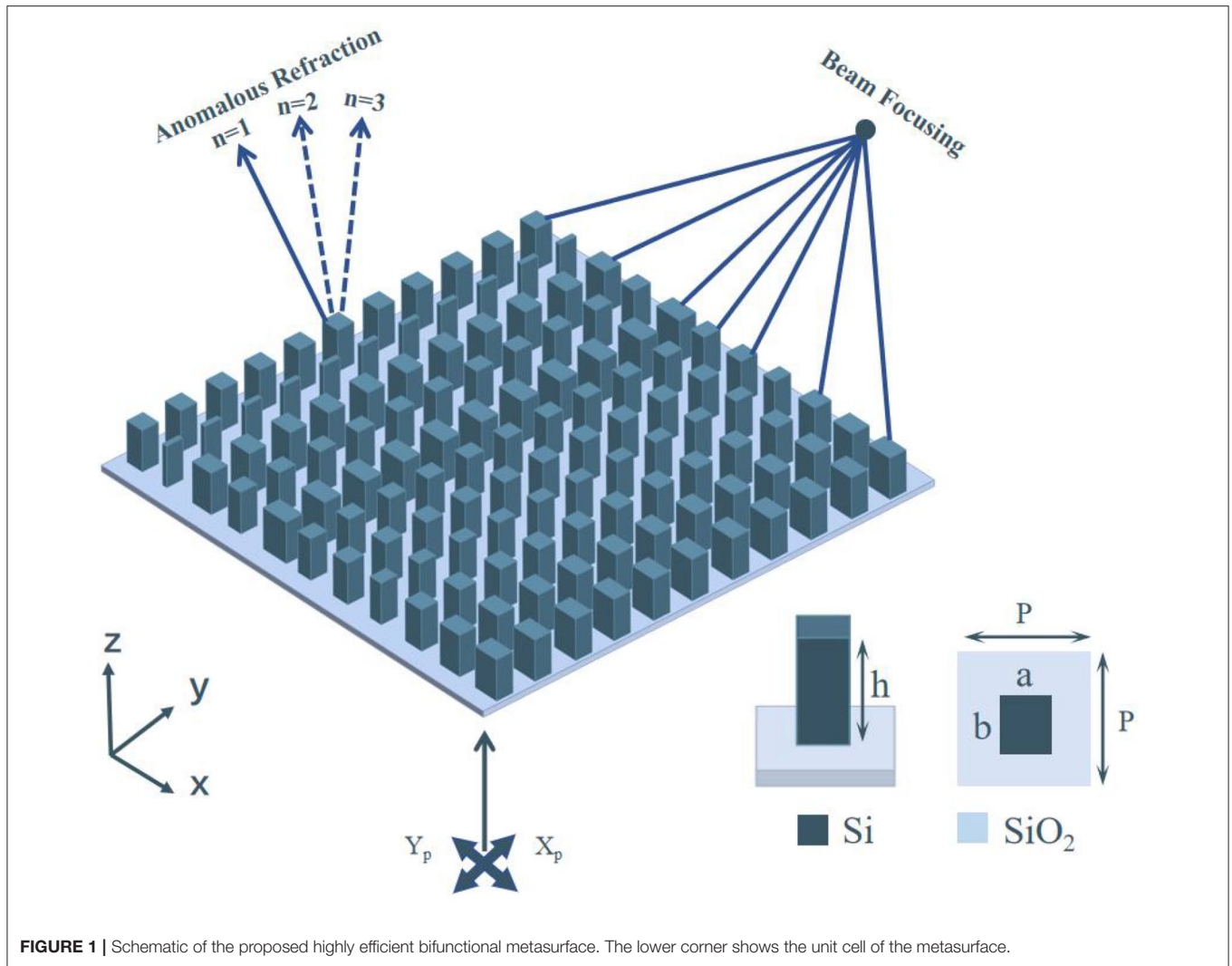


**FIGURE 1** | Schematic of the proposed highly efficient bifunctional metasurface. The lower corner shows the unit cell of the metasurface.

So far, most of metasurfaces invented by people have a single function. With the increasing demand for data storage and information management, it is desirable to fabricate a device that has multiple functions. Recently, metasurfaces with multiple functions have been developed by controlling the polarization, wavelength, and incident angle [18–23]. These metasurfaces can be used in integrated systems owing to their small footprint, which has been confirmed in the microwave [24, 25] and visible bands [26, 27]. Traditional bifunctional plasmonic metasurfaces mainly depend on the Pancharatnam-Berry (PB) phase to control the wavefront of circularly polarized (CP) light. In spite of its intrinsic wavelength-independent and dispersion-free features which results in the broadband operation, the PB phase is susceptible to several restrictions. For a metasurface that depends on the PB phase, the incident CP light is known to be scattered into waves of both the same and opposite polarizations [28]. By rotating the orientation of meta-atoms, it is easy to obtain the abrupt phase shift, which is useful for wavefront shaping. However, it works only for CP light with the opposite polarization, leading to a limited polarization

conversion efficiency of 25% [29]. Due to the metasurface is formed by spatial multiplexing of two metasurfaces that provide different functions, it may cause a functional crosstalk because one function tends to add background noise to the other [30].

In this paper, we propose a highly efficient bifunctional dielectric metasurface, enabling beam anomalous refraction and focusing at visible wavelength. The meta-atom constituting the metasurface unit cell is made of rectangular silicon nanopillar, enduing polarization-selective phase shifts to realize the two functions. With regard to this purpose, we first discussed the relationship between the geometric parameters of the nanopillar and the polarization-dependent phase shifts, the results show that, upon the light with the designated polarizations in normal incidence, the metasurface not only exhibits a highly efficient and ignorable functional crosstalk beam anomalous refraction, but also exhibits light focusing. Based on the metasurface proposed above, the other two metasurfaces demonstrating high-order beam anomalous refraction and focusing have been designed successfully. The reliability of the proposed method is

confirmed by the consistency between the simulation and theoretical calculation.

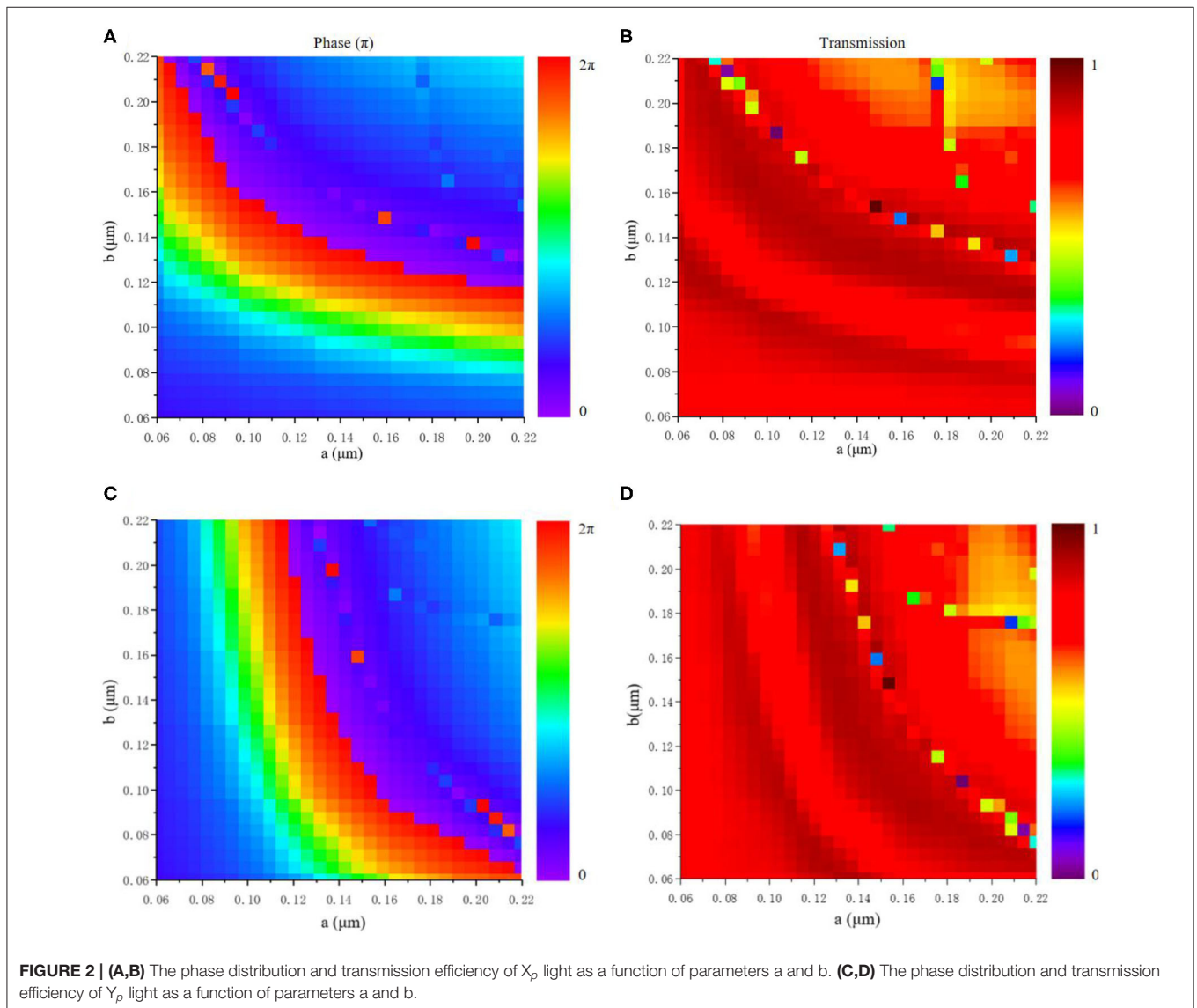
## DESIGN AND ANALYSIS

A bifunctional metasurface is required to impart two disparate spatial phase distributions efficiently to realize distinct wavefront modulation. Moreover, the two functions will not entail crosstalk, meaning that one function is rarely affected by the other. Our bifunctional metasurface is based on the idea that a single dielectric element atom causes a flexible phase delay on incident light according to polarization. The schematic of the proposed bifunctional metasurface is shown in **Figure 1**. For the incident light of X-linear-polarized ( $X_p$ ) and Y-linear-polarized ( $Y_p$ ), the metasurface can realize beam anomalous refraction and focusing, respectively. The dotted lines correspond to modes 2 and 3. The unit cell is composed of a rectangular Si nanopillar on the top of

a silicon dioxide ( $\text{SiO}_2$ ) substrate, as shown in the illustration in the lower right corner. The illustration shows the section and top views of the unit cell. Regarding the unit cell, the Si nanopillar implies a full range of phase from  $0$  to  $2\pi$  in the transmission of  $X_p$  and  $Y_p$  incident light, which can provide a full span of wavefront phase. To investigate the feasibility of the proposed design, we simulate the bifunctional metasurface using the finite difference time domain (FDTD) method (FDTD Solutions, Lumerical, Canada). In the simulations, the period of the unit cell is set as  $P = 230$  nm, while the thickness of Si nanopillars are set as  $h = 310$  nm. The operation wavelength is designed to be 660 nm for the wavelength of optical communication.

## RESULTS AND DISCUSSIONS

For the proposed dielectric metasurface, it is believed that the Si nanopillar constituting the unit cell plays a role as a truncated



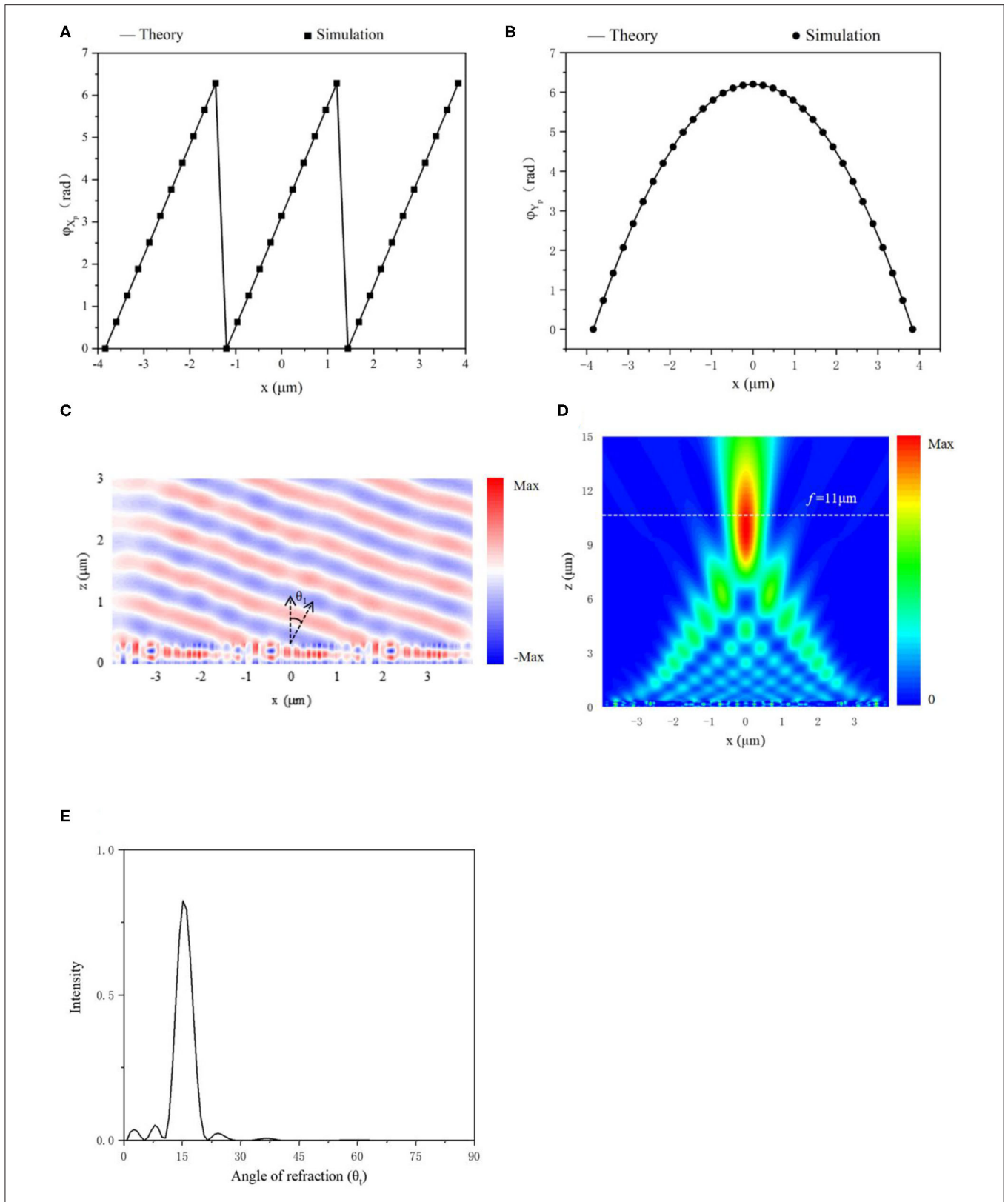


**FIGURE 3 | (A,B)** The theoretical and simulated phase profiles for beam anomalous refraction and focusing under normal  $X_p$  and  $Y_p$  light incidence, respectively. **(C)** The x-component of the transmitted electric field under normal  $X_p$  light incidence. **(D)** The y-component of the transmitted field intensity under normal  $Y_p$  light incidence. **(E)** Normalized far-field intensity as a function of the angle of refraction at the wavelength of  $\lambda = 660 \text{ nm}$  under normal  $X_p$  light incidence.

waveguide and operates as a low-quality factor Fabry-Pérot resonance [20]. **Figures 2A,B** exhibit the phase variations and transmission efficiency of  $X_p$  light, respectively, as a function of the widths of the nanopillar, including  $a$  and  $b$ . Similarly, **Figures 2C,D** correspond to  $Y_p$  light, and the efficiency has reached more than 86%.

A bifunctional metasurface composed of an array of  $33 \times 33$  meta-atoms has been proposed to realize beam anomalous refraction and focusing. In this regard, it is proved that a bifunctional metasurface that employs the proposed nanopillars can impart two different wavefront modulations. Each row of 33 nanopillars arranged along the  $x$ -axis can be considered as a supercell that imparts a hyperbolic phase distribution to the incidence of  $Y_p$  light. With regard to the anomalous refraction realized by the incidence of  $X_p$  light, the 33 nanopillars along the  $y$ -axis can be considered as three supercells, with each supercell consisting of 11 nanopillars to provide a linearly varying  $2\pi$  phase shift. Both theoretical and simulated phase profiles are demonstrated in **Figures 3A,B**. For the incidence of  $X_p$  light, the

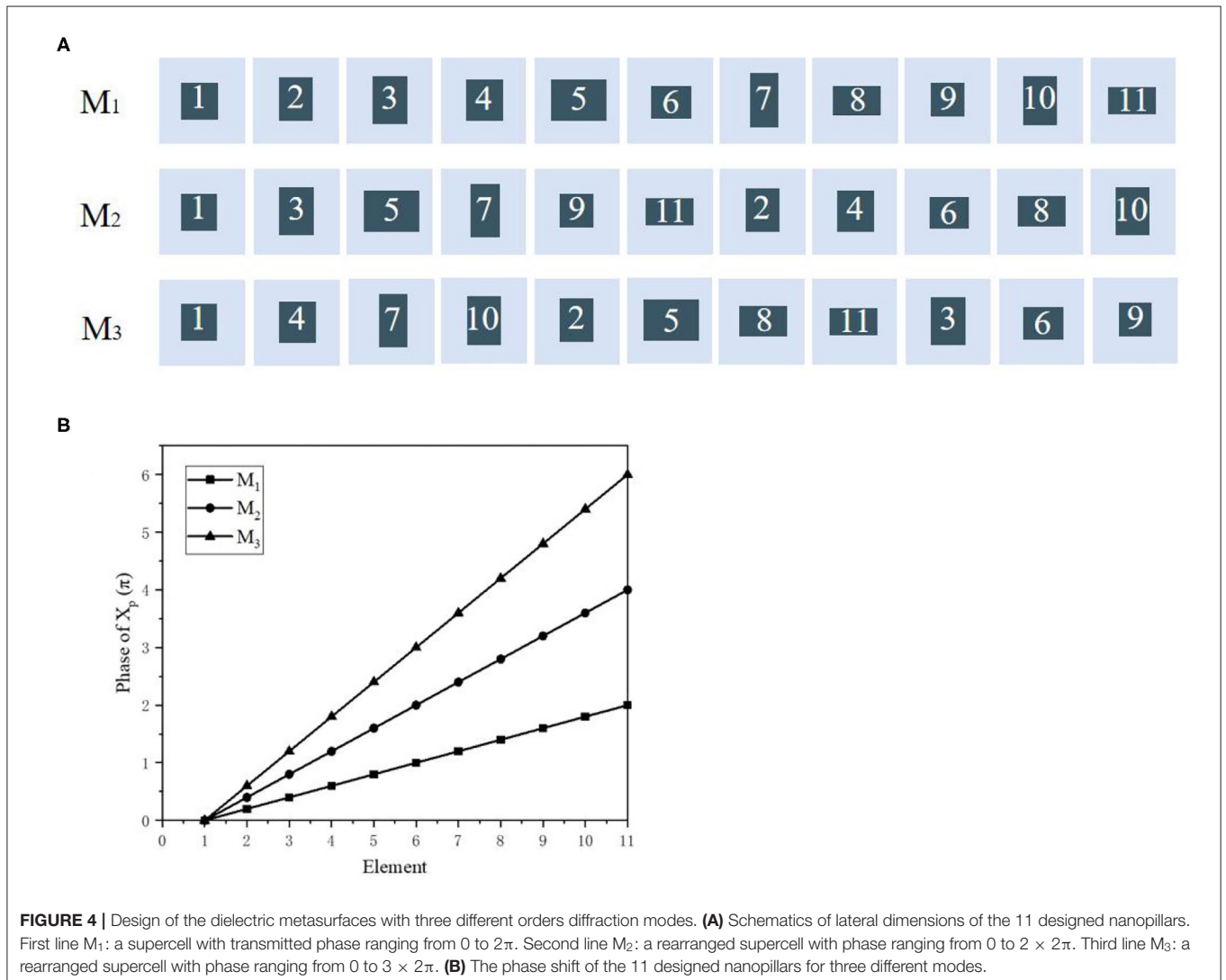
anomalous refraction is depicted in **Figure 3C**, and the phase profile of the anomalous refraction is dictated by the generalized Snell's law:

$$\sin(\theta_t)n_t - \sin(\theta_i)n_i = \frac{\lambda}{2\pi} \frac{d\Phi}{dx} \tag{1}$$

where  $\theta_i$  is the incident angle,  $n_i$  and  $n_t$  are the refractive indices of the incident and transmitting media, respectively, and  $d\Phi/dx$  is the gradient of phase discontinuity along the interface. For the incidence of  $Y_p$  light, the beam is focused at a focal length  $f$ , which is designed to be  $11 \mu\text{m}$ , as shown in **Figure 3D**. Its hyperbolic phase profile is governed by the following equation:

$$\phi(x) = \frac{2\pi}{\lambda} (f - \sqrt{(x - x_0)^2 + f^2}) \tag{2}$$

where  $\lambda$  is the operating wavelength, and  $x_0$  is the central position in the middle of the supercell. The angle of refraction  $\theta_t$  is



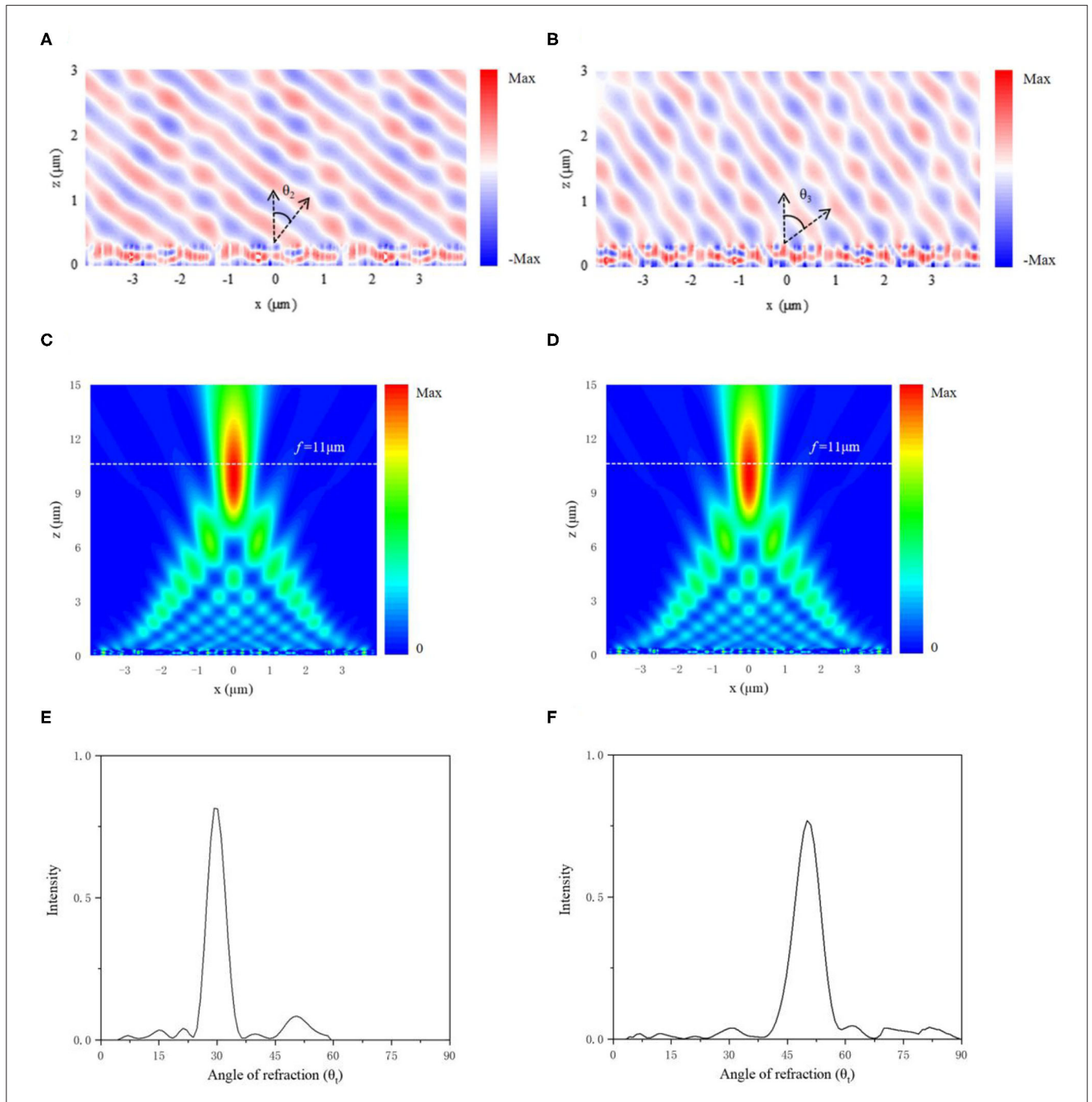


**FIGURE 5 | (A,B)** The x-component of the transmitted electric field under normal  $X_p$  light incidence on the metasurface working in the 2nd and 3rd orders, respectively. **(C,D)** The y-component of the transmitted field intensity under normal  $Y_p$  light incidence on the metasurface working in the 2nd and 3rd orders, respectively. **(E,F)** Normalized far-field intensity as a function of the angle of refraction at the wavelength of  $\lambda = 660 \text{ nm}$  under normal  $X_p$  light incidence on the metasurface working in the 2nd and 3rd orders, respectively.

estimated to be  $14.02^\circ$  in simulation (Figure 3E), which closely agrees with the theoretically calculated angle of  $14.48^\circ$ .

Based on the designed metasurface above, two metasurfaces working in high-order diffraction modes have been designed successfully. In the design of metasurface 1 ( $M_1$ ), we discrete the

phase range from 0 to  $2\pi$  to 0 into 11 nanopillars along the y-axis with equal step of  $\pi/5$  for  $X_p$  transmitted light. The lateral dimensions of the 11 selected silicon nanopillars are numbered in ascending order, as shown in the first line of Figure 4A. It appears that the range of phase control could be extended to

high-order diffraction modes by appropriately selecting the unit cells in  $M_1$  and rearranging them. For instance, if we intend to expand the diffraction mode to the  $N$ th order, the phase coverage should be from 0 to  $N \times 2\pi$  with a gradient of  $N \times \pi/5$  between two neighboring nanopillars for  $X_p$  transmitted light. As a result, the second line of **Figure 4A** presents the rearranged supercell for the second order diffraction mode ( $M_2$ ), where the phase coverage of the unit cell is from 0 to  $4\pi$  with a gradient of  $2\pi/5$  between two neighboring nanopillars for  $X_p$  transmitted light. Similarly, a metasurface working in the third order diffraction mode is also constructed by a set of 11 dielectric nanopillars, whose phase coverage is from 0 to  $6\pi$  with a gradient of  $3\pi/5$  between two neighboring nanopillars for  $X_p$  transmitted light, as shown in the third line of **Figure 4A**. To clearly outline the concept, we plot the transmission phase of the 11 elements with three concrete arrangements for  $X_p$  transmitted light, as shown in **Figure 4B**.

For comparison, **Figure 5** demonstrates the beam anomalous refraction and focused electric field distribution of the other two rearranged metasurfaces made of newly designed supercells ( $M_2$  and  $M_3$ ) for  $X_p$  and  $Y_p$  incident light. Since the supercells of the two metasurfaces have been rearranged, the optical behavior of  $M_2$  and  $M_3$  are governed by the following diffraction equation:

$$\sin(\theta_t)n_t - \sin(\theta_i)n_i = m \frac{\lambda}{D} \quad (3)$$

where  $m$  is the order of diffraction spectrum, and  $D = 11p$  is the periodicity of the supercell. According to Equations (1) and (3), it can be noted that the interface with the phase coverage of  $2 \times 2\pi$  and  $3 \times 2\pi$ , correlates to  $d\Phi/dx = 2 \times 2\pi/D$  and  $d\Phi/dx = 3 \times 2\pi/D$ , respectively, over a periodicity  $D$ , the resulting anomalous refraction corresponds to the second and third order diffraction. The effect of focusing will not be affected due to the phase of the supercell along the  $x$ -axis is in maintaining with the metasurface working in the first-order diffraction. **Figures 5A,C** show that the metasurface working in the second order has an anomalous refraction angle  $\theta_2$  and the beams are focused at  $11 \mu\text{m}$ , **Figure 5B,D** correspond to the third order. It is clearly obtained from **Figures 5E,F** that the angles of refraction  $\theta_2$  and

$\theta_3$  are  $29.58^\circ$  and  $48.43^\circ$ , respectively, which are closely consistent with the theoretically calculated angles of  $30^\circ$  and  $48.59^\circ$ .

## CONCLUSION

In conclusion, we have proposed a highly efficient transmissive bifunctional metasurface that enables the beam anomalous refraction and focusing at visible wavelength. By controlling the parameters of the Si nanopillars in each unit cell of the metasurface, a full range of phase from 0 to  $2\pi$  for the transmission of incident light and a high efficiency (over 86%) are obtained. The nanopillars that comprise the bifunctional metasurface are devised accurate to impart a linear and hyperbolic phase profile to the  $X_p$  and  $Y_p$  incident lights, respectively. Based on the designed metasurface, another two metasurfaces that demonstrate the high-order beam anomalous refraction and focusing have been proposed successfully. Our work can be easily extended to the design of other optical transmitting facilities with high-efficiency, which will be useful in the fabrication of miniaturized and multifunctional metadevices.

## DATA AVAILABILITY STATEMENT

The original contributions presented in the study are included in the article/supplementary material, further inquiries can be directed to the corresponding author.

## AUTHOR CONTRIBUTIONS

All the authors designed research, performed research, analyzed data, and wrote the paper.

## FUNDING

This work was supported by the National Natural Science Foundation of China (Grant Nos. 61705127, 11704243) and Degree construction project of Detection Technology and Automation Devices of Shanghai University of Engineering Science (No. 19XXK003).

## REFERENCES

1. Yu N, Genevet P, Kats MA, Aieta F, Tetienne JP, Capasso F, et al. Light propagation with phase discontinuities: generalized laws of reflection and refraction. *Science*. (2011) **334**:333–7. doi: 10.1126/science.1210713
2. Veselago VG. The electrodynamics of substances with simultaneously negative values of  $\epsilon$  and  $\mu$ . *Sov Phys Usp*. (1968) **10**:509–14. doi: 10.1070/PU1968v010n04ABEH003699
3. Wang W, Guo Z, Zhou K, Sun Y, Shen F, Li Y, et al. Polarization-independent longitudinal multi-focusing metalens. *Opt Express*. (2015) **23**:29855–66. doi: 10.1364/OE.23.029855
4. Li Z, Palacios E, Butun S, Aydin K. Visible-frequency metasurfaces for broadband anomalous reflection and high-efficiency spectrum splitting. *Nano Lett*. (2015) **15**:1615–21. doi: 10.1021/nl5041572
5. Lyer PP, Butakov NA, Schuller JA. Reconfigurable semiconductor phased-array metasurfaces. *ACS Photonics*. (2015) **2**:1077–84. doi: 10.1021/acsp Photonics.5b00132
6. Colburn S, Zhan A, Bayati E, Whitehead J, Ryou A, Huang L. Broadband transparent and CMOS-compatible flat optics with silicon nitride metasurfaces. *Opt Mater Express*. (2018) **8**:2330–34. doi: 10.1364/OME.8.002330
7. Shang X, Meeus L, Cuypers D. Fast switching cholesteric liquid crystal optical beam deflector with polarization independence. *Sci Rep*. (2017) **7**:6492. doi: 10.1038/s41598-017-06944-z
8. Ni X, Emani NK, Kildishev AV, Boltasseva A, Shalaev VM. Broadband light bending with plasmonic nanoantennas. *Science*. (2012) **335**:427. doi: 10.1126/science.1214686
9. Li Z, Huang L, Lu K, Sun Y, Min L. Continuous metasurface for high-performance anomalous reflection. *Appl Phys Express*. (2014) **7**:112001. doi: 10.7567/APEX.7.112001
10. Li Z, Cai X, Huang L, Xu H, Dai N. Controllable polarization rotator with broadband high transmission using all-dielectric metasurface. *Adv Theory Simul*. (2019) **2**:1900086. doi: 10.1002/adts.201900086

11. Arbabi E, Arbabi A, Kamali SM, Horie Y, Faraon A. Multiwavelength polarization-insensitive lenses based on dielectric metasurfaces with meta-molecules. *Optica*. (2016) 3:628–33. doi: 10.1364/OPTICA.3.000628
12. Li R, Guo Z, Wang W, Zhang J, Zhou K, Liu J, et al. Arbitrary focusing lens by holographic metasurface. *Photonics Res.* (2015) 3:252–5. doi: 10.1364/PRJ.3.000252
13. Bayati E, Zhan A, Colburn S, Zhelyeznyakov MV, Majumdar A. Role of refractive index in metals performance. *Appl Opt.* (2019) 58:1460–66. doi: 10.1364/AO.58.001460
14. Hao J, Yuan Y, Ran L, Jiang T, Kong JA, Chan CT, et al. Manipulating electromagnetic wave polarizations by anisotropic metamaterials. *Phys Rev Lett.* (2007) 99:063908. doi: 10.1103/PhysRevLett.99.063908
15. Li Y, Li Z, Liu Y, Kong Y, Huang L. Broadband and highly polarization conversion in infrared region using plasmonic metasurfaces. *Opt Mater.* (2019) 98:109420. doi: 10.1016/j.optmat.2019.109420
16. Chen W, Yang KY, Wang CM, Huang YW, Sun G, Chiang ID, et al. High-efficiency broadband meta-hologram with polarization-controlled dual images. *Nano Lett.* (2014) 14:225–30. doi: 10.1021/nl403811d
17. Wang B, Dong F, Li QT, Yang D, Sun C, Chen J, et al. Visible-frequency dielectric metasurfaces for multiwavelength and highly dispersive holograms. *Nano Lett.* (2016) 16:5235–40. doi: 10.1021/acs.nanolett.6b02326
18. Pors A, Albrektsen O, Radko IP, Bozhevolnyi SI. Gap plasmon-based metasurfaces for total control of reflected light. *Sci Rep.* (2013) 3:2155. doi: 10.1038/srep02155
19. Farmahini-Farahani M, Mosallaei H, Birefringent reflectarray metasurface for beam engineering in infrared. *Opt Lett.* (2013) 38:462–4. doi: 10.1364/OL.38.000462
20. Arbabi A, Horie Y, Bagheri M, Faraon A. Dielectric metasurfaces for complete control of phase and polarization with subwavelength spatial resolution and high transmission. *Nat Nanotechnol.* (2015) 10:937–43. doi: 10.1038/nnano.2015.186
21. Chen Y, Yang X, Gao J. Spin-controlled wavefront shaping with plasmonic chiral geometric metasurface. *Light.* (2018) 7:84. doi: 10.1038/s41377-018-0086-x
22. Li Z, Hao J, Huang L, Li H, Xu H, Sun Y, et al. Manipulating the wavefront of light by plasmonic metasurfaces operating in high order modes. *Opt Express.* (2016) 24:8788–96. doi: 10.1364/OE.24.008788
23. Khan MI, Fraz Q, Tahir FA. Ultra-wideband cross polarization conversion metasurface insensitive to incidence angle. *J Appl Phys.* (2017) 121:045103. doi: 10.1063/1.4974849
24. Cai T, Tang S, Wang G, Xu H, Sun S, He Q, et al. High-performance bifunctional metasurfaces in transmission and reflection geometries. *Adv Opt Mater.* (2016) 5:1600506. doi: 10.1002/adom.201600506
25. Cai T, Wang G-M, Xu H-X, Tang S-W, Li H, Liang J-L, et al. Bifunctional pancharatanam-berry metasurface with high-efficiency helicity-dependent transmissions and reflection. *Ann Phys.* (2017) 530:1700321. doi: 10.1002/andp.201700321
26. Shi Z, Khorasaninejad M, Huang YW, Roques-Carmes C, Zhu AY, Chen WT, et al. Single-layer metasurface with controllable multiwavelength functions. *Nano Lett.* (2018) 18:2420–7. doi: 10.1021/acs.nanolett.7b05458
27. Zhang C, Yue F, Wen D, Chen M, Zhang Z, Wang W, et al. Multichannel metasurface for simultaneous control of holograms and twisted light beams. *ACS Photonics.* (2017) 4:1906–12. doi: 10.1021/acsp Photonics.7b00587
28. Huang L, Chen X, Mühlenbernd H, Li G, Bai B, Tan Q, et al. Dispersionless phase discontinuities for controlling light propagation. *Nano Lett.* (2012) 12:5750–55. doi: 10.1021/nl303031j
29. Liu C, Bai Y, Zhao Q, Yang Y, Chen H, Zhou J, et al. Fully controllable pancharatanam-berry metasurface array with high conversion efficiency and broad bandwidth. *Sci Rep.* (2016) 6:34819. doi: 10.1038/srep34819
30. Avayu O, Almeida E, Prior Y, Ellenbogen T. Composite functional metasurfaces for multispectral achromatic optics. *Nat Commun.* (2017) 8:14992. doi: 10.1038/ncomms14992

**Conflict of Interest:** The authors declare that the research was conducted in the absence of any commercial or financial relationships that could be construed as a potential conflict of interest.

Copyright © 2020 Xu, Li, Tian, Wei and Wu. This is an open-access article distributed under the terms of the Creative Commons Attribution License (CC BY). The use, distribution or reproduction in other forums is permitted, provided the original author(s) and the copyright owner(s) are credited and that the original publication in this journal is cited, in accordance with accepted academic practice. No use, distribution or reproduction is permitted which does not comply with these terms.